JOURNAL OF GEOPHYSICAL RESEARCH, VOL. 113, C02018, doi:10.1029/2007JC004429, 2008

Age characteristics of a shelf-break eddy in the western Arctic and implications for shelf-basin exchange

David Kadko,[1] Robert S. Pickart,[2] and Jeremy Mathis[1]

Received 1 July 2007; revised 24 October 2007; accepted 21 November 2007; published 22 February 2008.

[1] Radioisotope evaluation of a cold-core, anticyclonic eddy surveyed in September 2004 on the Chukchi Sea continental slope was used to determine its age since formation over the shelf environment. Because the eddy can be shown to have been generated near the shelf break, initial conditions for several age-dependent tracers could be relatively well constrained. A combination of $^{228}Ra/^{226}Ra$, excess ^{224}Ra, and $^{228}Th/^{228}Ra$ suggested an age on the order of months. This age is consistent with the presence of elevated concentrations of nutrients, organic carbon, suspended particles, and shelf-derived neritic zooplankton within the eddy compared to ambient offshore water in the Canada Basin but comparable to values measured in the Chukchi shelf and shelf-break environment. Hence this feature, at the edge of the deep basin, was poised to deliver biogeochemically significant shelf material to the central Arctic Ocean.

Citation: Kadko, D., R. S. Pickart, and J. Mathis (2008), Age characteristics of a shelf-break eddy in the western Arctic and implications for shelf-basin exchange, *J. Geophys. Res.*, *113*, C02018, doi:10.1029/2007JC004429.

1. Introduction

[2] Pacific waters entering the Arctic Ocean through Bering Strait play important roles in maintaining the physical and biological regimes of the Arctic. These waters help ventilate the Arctic halocline, deliver nutrients essential for Arctic ecosystems, and contribute to the freshwater balance of the Arctic Ocean [e.g., *Cooper et al.*, 1997; *Woodgate et al.*, 2005]. The mean northward flow through Bering Strait is driven by large-scale sea level differences between the Bering and Chukchi Seas [*Coachman and Aagaard*, 1966]. Observations and modeling results suggest that upon reaching the edge of the Chukchi shelf, this flow is subsequently constrained by geostrophic dynamics to turn eastward following the isobaths [*Münchow et al.*, 2000; *Winsor and Chapman*, 2004; *Weingartner et al.*, 2005; *Spall*, 2007]. These dynamics which result in a shelf-edge current and hydrographic front prevent these waters from readily moving into deeper water. Thus cross-shelf transport is inhibited, as illustrated for example by the distribution of short-lived radium isotopes which have a shelf source function and display a sharp gradient across the Chukchi-Beaufort shelf break [*Hansell et al.*, 2004; *Kadko and Muench*, 2005].

[3] There are several mechanisms which are capable of overcoming this barrier at the shelf break leading to exchange across the Arctic shelf and slope. These include dense water plumes, wind induced upwelling/downwelling, and frontal instabilities which form eddies [*D'Asaro*, 1988a; *Muench et al.*, 2000; *Pickart et al.*, 2005]. Such processes conspire to ventilate the Arctic halocline on decadal timescales [*Aagaard and Carmack*, 1994]. Eddy formation and transport may be important in this regard because it is believed that the southern Canada Basin is populated at any time with 100–200 small-scale eddies [*Newton et al.*, 1974; *Manley and Hunkins*, 1985; A. J. Plueddemann and R. Krishfield, Physical properties of eddies in the western Arctic, submitted to *Journal of Geophysical Research*, 2008] composed of Pacific-origin water via the Chukchi Sea [*Muench et al.*, 2000; *Pickart et al.*, 2005; *Mathis et al.*, 2007]. Cold-core anticyclonic eddies observed seaward of the Chukchi-Beaufort shelf break have properties of the winter-transformed Bering water described by *Pickart et al.* [2005] and are in the salinity range required to ventilate the Canada Basin upper halocline. If a typical eddy volume is 25 km^3 and has a lifetime of 1 year, then a yearly flux of water from the shelf to the basin by 100–200 eddies would be sufficient to ventilate the halocline on a decadal timescale [e.g., *Pickart et al.*, 2005].

[4] Numerous studies have suggested that eddies deliver a substantial volume of water to the Canada Basin interior [e.g., *Manley and Hunkins*, 1985; *D'Asaro*, 1988a, 1988b; *Muench et al.*, 2000; *Pickart et al.*, 2005], and it is likely that there is an associated flux of substances critical to biogeochemical cycles, such as nutrients, silicate and carbon [*Muench et al.*, 2000; *Pickart et al.*, 2005; *Mathis et al.*, 2007]. However, to adequately evaluate the impact of the eddy flux in the export budget of water and material from the shelf, an understanding of the eddy lifetimes is required. For example, calculation of the export of biogeochemically significant shelf material to the deep basin via eddies requires knowing the "age" of the eddy. This would allow

[1] Rosenstiel School of Marine and Atmospheric Science, University of Miami, Miami, Florida, USA.
[2] Woods Hole Oceanographic Institution, Woods Hole, Massachusetts, USA.

0148-0227/08/2007JC004429$09.00

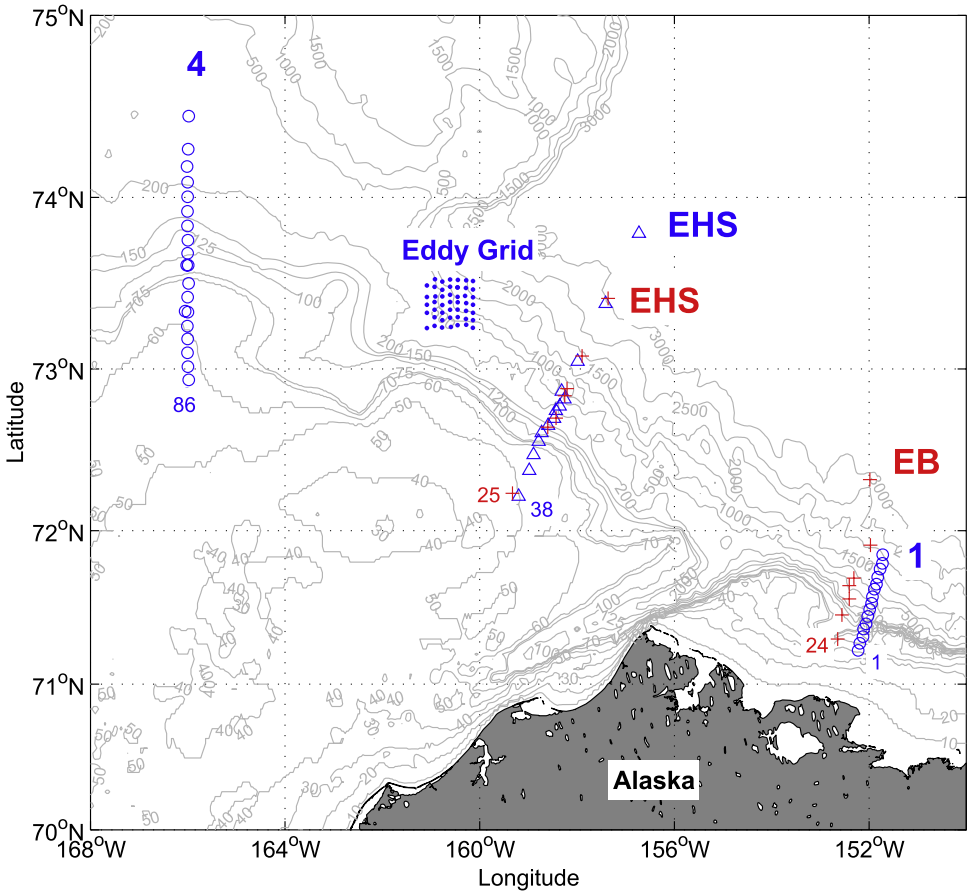

Figure 1. Locations of the hydrographic stations used in the analysis. Blue (red) represents stations occupied in summer 2004 (2002). Transects 1 and 4 (blue circles) were occupied in September 2004 (HLY-04-04). Transects EHS (East Hannah Shoal, red crosses, blue triangles) and EB (East Barrow, red crosses) are also shown. The station number of the southernmost site on each transect is labeled in small font to help orient the reader for subsequent figures. The XCTD stations (blue dots) comprising the eddy survey are shown as well.

characterization of a "newly formed" eddy; one which represents initial conditions prior to biogeochemical processing and thus the true potential for mass transport from the shelf and ultimate impact on the regional ecosystem. In addition, eddy lifetime in part determines the ability of eddies to ventilate the western Arctic; the longer an eddy stays intact, the greater chance it has of being advected far from its shelf source and even leaving the Canada Basin, thereby diminishing the contribution of the eddies to western Arctic ventilation.

[5] There have been few estimates of eddy age. *Padman et al.* [1990] used an observed rate of energy dissipation to derive a 10-year decay time for an Arctic cyclonic eddy, but pointed out that this calculation neglects possible episodic, higher energy mixing events which could result in a much shorter timescale. *Muench et al.* [2000], based in part on its calculated tritium-helium age, suggested that an anticyclonic Arctic eddy was over a year old; however it has recently been suggested that this age could be an overestimate because of incomplete atmospheric equilibration of the tracer [*Pickart et al.*, 2005]. In a study of Gulf Steam warm-core rings, excesses within some rings of the short-lived, naturally occurring ^{222}Rn suggested very rapid offshore transport (days) of waters that had been in contact with sediments and subsequently entrained within the rings [*Orr et al.*, 1985].

[6] In this work we present age estimates of a cold-core, anticyclonic eddy surveyed in September 2004 on the Chukchi continental slope. Because the waters comprising the eddy can be shown to have originated from the shelf environment, initial conditions for several age-dependent tracers can be relatively well constrained allowing the age of the eddy to be estimated.

2. Methods

[7] In September 2004 a detailed hydrographic survey was conducted of an anticyclonic, cold-core eddy located on the Chukchi continental slope. The survey was carried out during the USCGC *Healy* cruise HLY-04-04 as part of the western Arctic Shelf-Basin Interactions Program (SBI) (Figure 1). The eddy was first located using expendable bathythermographs (XBTs) then sampled with a finely spaced grid of conductivity/temperature/depth measurements (CTDs) from both shipboard casts (extending to 300 m) and expendable XCTDs. The resolution of the grid was roughly 5 km (Figure 1), and the survey took approximately 24 hours to complete [see also *Mathis et al.*, 2007].

Immediately following the high-resolution physical sampling, a hydrographic transect was taken through the center of the feature in order to obtain samples for biological, chemical and radioisotope analyses of the eddy.

[8] The shipboard CTD used was a Seabird 911+ with dual temperature and conductivity sensors. The accuracy of the temperature measurement was estimated to be 0.001°C on the basis of precruise laboratory calibrations and comparison between the two sensors. The conductivity was calibrated using in situ water sample data collected at the deep stations during the cruise. On the basis of this, the estimated salinity accuracy for the depth range of the eddy is 0.007. The type of XCTD probe used in the survey was Sippican model 1. As a check on the stated accuracy of these probes, we dropped one of the XCTDs coincident with a CTD cast (this was done only once because of constraints on time and resources). The comparison was extremely favorable as the CTD and XCTD measured the identical features (not shown). Detailed comparison of the two casts indicates that the XCTD was biased by −0.038 in salinity, 0.02°C in temperature, and 0.04 m in depth (the standard deviation of the difference in depth was 0.75 m) relative to the calibrated shipboard CTD. These are all within the stated accuracy of the XCTD probe. Hence we take the XCTD temperature, salinity, and depth accuracies during the eddy survey to be 0.02°C, 0.04, and approximately 1 m, respectively.

[9] Samples for radium isotopes were also collected during the SBI cruises HLY-02-03 in July–August 2002 and HLY-04-03 in July–August 2004. Throughout the SBI program, these samples were collected from Niskin bottles and emptied into 50-gallon plastic drums that were then slowly drained with electric pumps (∼1 l/min) through plastic tubes packed with manganese-coated acrylic fibers. It has been shown that these fibers adsorb radium isotopes efficiently and without fractionation [*Moore et al.*, 1985]. Immediately after drainage, each fiber was placed in a stripping line, and ^{224}Ra was determined by counting its daughter ^{220}Rn ($T_{1/2}$ = 55.6 s). Within a closed circulation loop, ^{220}Rn was stripped by helium directly into a ZnS coated, scintillation cell/photomultiplier delayed coincidence counting system [*Moore and Arnold*, 1996]. The efficiency of the system is determined by a ^{228}Th (parent of ^{224}Ra) standard. This procedure is replicated over a period of several weeks to determine the ^{228}Th activity of the sample. On land, the fibers were sealed in plastic petrie dishes then counted by gamma spectrometry using established procedures to determine the ^{228}Ra/^{226}Ra ratios [e.g., *Michel et al.*, 1981; *Rutgers van der Loeff et al.*, 1995, 2003; *Kadko and Muench*, 2005].

3. Results and Discussion

3.1. Eddy Characteristics

[10] The eddy feature, centered at a depth of ∼150 m, had a diameter of 16 km and was situated on the continental slope between the 500 and 1500 m isobaths (Figures 2 and 3). It was a cold-core anticyclone (potential temperature < −1.7°C), with a thickness > 90 m at its center (Figure 2). The range in density was approximately 26.4–26.8 kg m^{-3} and that of salinity 32.8–33.3, which is characteristic of water capable of ventilating the upper halocline of the interior Canada Basin [e.g., *Cooper et al.*, 1997; *Pickart et al.*, 2005]. This is the same type of feature that *Muench et al.* [2000] sampled in the deep Canada Basin, and that *Pickart et al.* [2005] observed being spawned from the shelf-edge current of the Chukchi Sea west of Barrow Canyon (in this same region) during the summer season. It is likely therefore that the eddy observed here was formed in similar fashion, possibly from baroclinic instability of the shelf-edge current [see *Pickart et al.*, 2005; *Spall et al.*, 2008].

[11] The chemistry and zooplanktonic assemblage of the feature have been described elsewhere [*Mathis et al.*, 2007; *Llinás et al.*, 2008]. Briefly, it was found that concentrations of nutrients, organic carbon, and suspended particles within the eddy were elevated compared to surrounding, ambient offshore water in the Canada Basin, but comparable to values measured in the vicinity of the shelf and shelf break during the SBI program. Similarly, the eddy was enriched in the coastal neritic zooplankton species *Pseudocalanus* compared to the surrounding ambient water. In addition, the core of the eddy contained copepods (*Neocalanus flemingeri* and *Metridia pacifica*) from the Bering Sea [*Llinás et al.*, 2008]. These data support the suggestion that interaction of dense, winter transformed Pacific-origin water with shelf sediments results in entrainment of remineralized nutrients and organic carbon [*Cooper et al.*, 1997; *Mathis et al.*, 2007]. It follows that eddies formed in this environment, and subsequently transferred offshore, could be a significant mechanism for delivering these properties to the interior of the Canada Basin. Figure 4 shows the potential temperature and particle content (percent light transmission) from transect 4 of the September 2004 HLY-04-04 cruise (see Figure 1 for location). The low temperatures and reduced transmission in the vicinity of the shelf break are indicative of the spring/summer configuration of the shelf-edge current [*Pickart et al.*, 2005]. Figure 5 from transect EB (East of Barrow, equivalent to transect 1 near 152°W in Figure 1) in summer 2002 shows the general observation in the western Arctic of a higher percentage of river water away from the nearshore as the deep basin is approached. This situation is unlike that normally found at lower latitudes, where fresher waters are on the shelf. This unique distribution results from the inflow of Pacific water to the shelf through Bering Strait, and the introduction of largely Mackenzie River water to the offshore east of the study region [*Macdonald et al.*, 1999; *Hansell et al.*, 2004; *Kadko and Muench*, 2005]. These results derive from partitioning of the water from end-member analysis based on δ^{18}O and salinity content [e.g., *Macdonald et al.*, 1995, 1999; *Kadko and Swart*, 2004]. Hence water trapped within an eddy spawned from the shelf-break current in the vicinity of the Chukchi Sea would be expected to have lower temperature, higher particle content (lower light transmission), and a smaller river water component than water offshore. Data from the hydrographic section taken through the center of the eddy (see Figure 2 for transect location) indicate that these characteristics were indeed observed within the eddy (Figure 6). Such correspondence between parameters measured nearshore along the shelf-

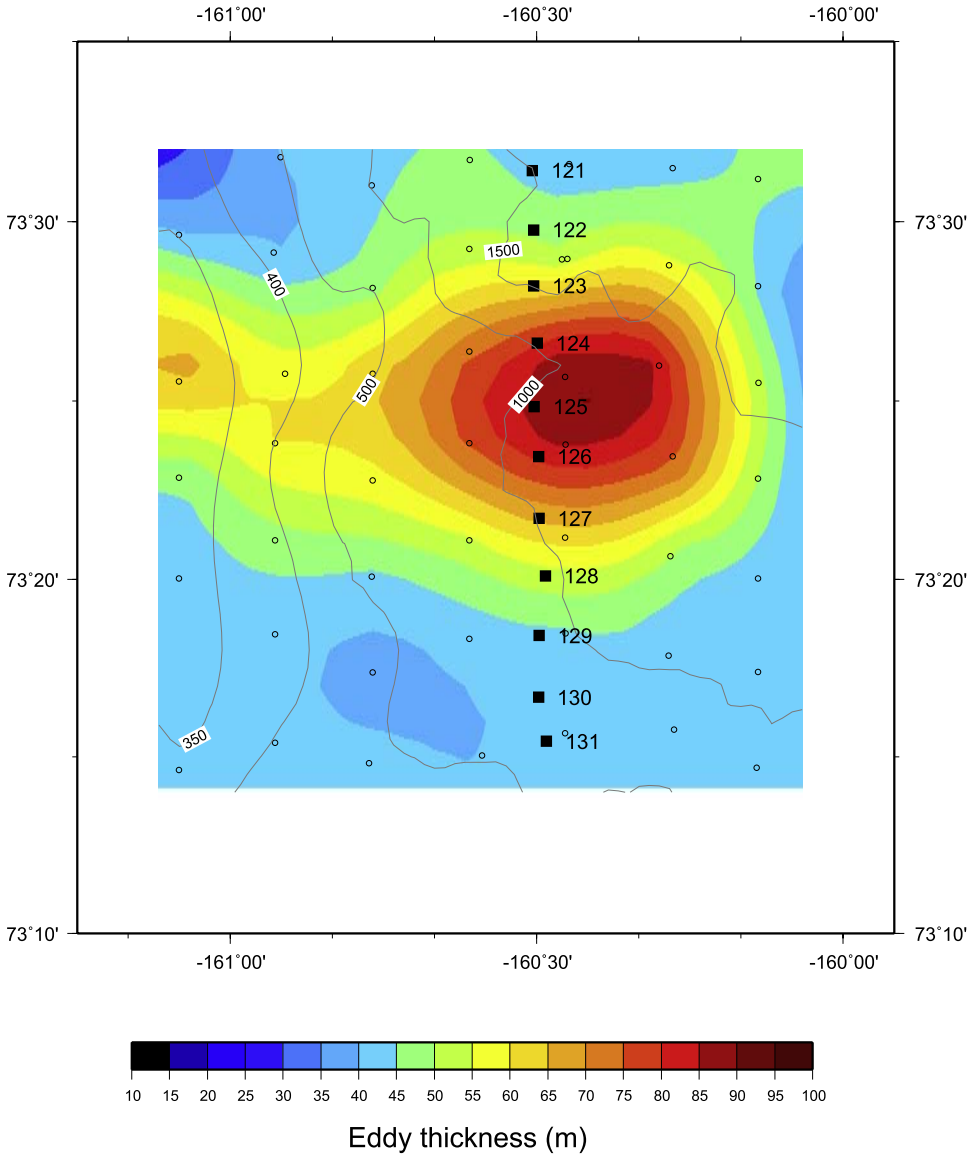

Figure 2. Map view of the eddy showing its thickness, as defined by the bounding density surfaces 26.4 and 26.8 kg m^{-3}. The locations of the XCTD and CTD measurements comprising the high-resolution grid are indicated by the open circles. The stations corresponding to the hydrographic transect with water samples (stations 121–131) are denoted by the solid black squares. Bottom depth (from the ship's multibeam system) is contoured in meters.

break transect and the eddy does not imply knowledge of the exact source location, or the timing of the eddy formation, but is consistent with the general mode and location of eddy formation in this region as discussed elsewhere [e.g., *Pickart et al.*, 2005; *Mathis et al.*, 2007; *Spall et al.*, 2008].

3.2. Radium Tracers

[12] As a result of interaction of the eddy source water with shelf sediments, the water also becomes enriched in radium isotopes produced in the sediments (Figure 7). Here we utilize two radium isotopic techniques to estimate the age-since-formation of the eddy observed in 2004. The analytical results are presented for the eddy survey and transects 1 and 4 from the September 2004 cruise HLY-04-04 in Table 1. Data from the nearby transect East Hannah Shoal (EHS, location in Figure 1) for earlier SBI cruises HLY-02-03 (July–August 2002) and HLY-04-03 (July–August 2004) are presented in Tables 2 and 3.

3.2.1. The Ratio $^{228}Ra/^{226}Ra$

[13] The ratio of two isotopes of radium, ^{228}Ra ($T_{1/2}$ = 5.77 years) and ^{226}Ra ($T_{1/2}$ = 1620 years) have been used as tracers of sediment-water interaction and shelf-basin exchange in the Arctic [*Rutgers van der Loeff et al.*, 1995, 2003; *Hansell et al.*, 2004; *Kadko and Muench*, 2005]. Radium is derived from the decay of thorium in the sediments. Radium-228 is produced from the decay of ^{232}Th, and ^{226}Ra from the decay of ^{230}Th. Because radium is mobile in sediment pore water, a fraction of the radium

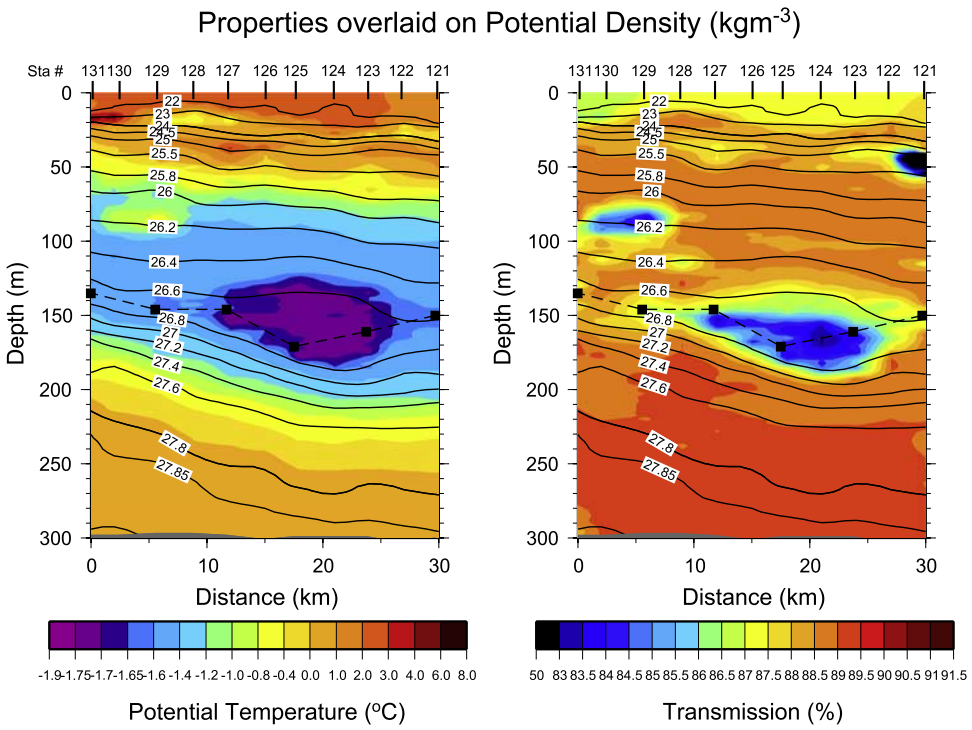

Figure 3. Vertical property sections through the eddy, from the hydrographic transect occupied at the conclusion of the high-resolution survey (see Figure 2 for location of the transect relative to the eddy). (left) Potential temperature (color) overlaid with potential density (contours). (right) Percent light transmission (color) overlaid with potential density (contours). The water sample locations for the data presented in Figure 8 are indicated by the black squares.

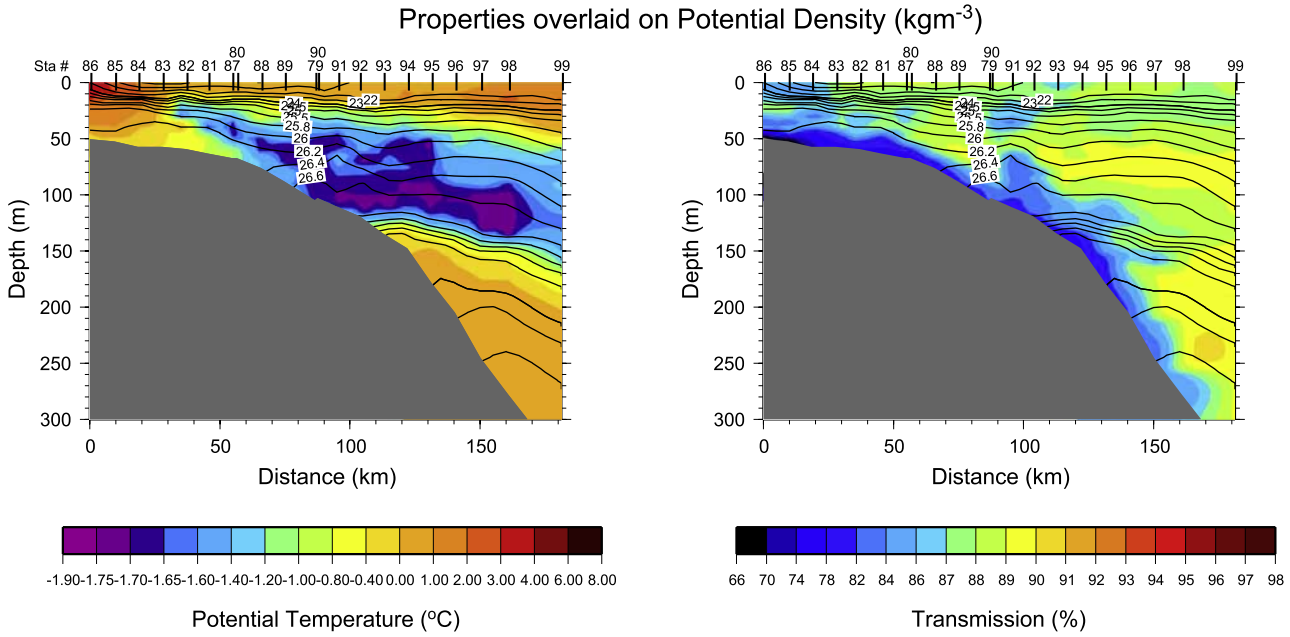

Figure 4. Vertical property sections for transect 4 occupied during the September 2004 USCGC *Healy* cruise HLY-04-04 (see Figure 1 for location). (left) Potential temperature (color) overlaid with potential density (contours). (right) Transmission (color) overlaid with potential density (contours). The low temperature and high particle content in the vicinity of the shelf break are consistent with the eddy properties. The oxygen concentration for this transect is shown in Figure 12a.

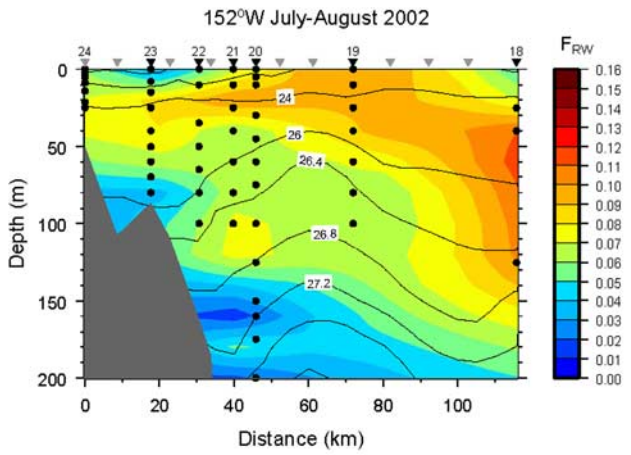

Figure 5. Fraction of river water (color) based on $\delta^{18}O$ and salinity analyses, overlaid with potential density (contours), for the summer 2002 occupation of transect EB (near 152°W). The sample depths are marked by the black circles. The black numbered inverted triangles denote the CTD stations, and the grey inverted triangles denote the XCTD sites. Note the generally higher F_{RW} offshore.

produced there diffuses into the overlying water. Therefore Ra isotope enrichment occurs in marine waters when they contact sediment, and waters crossing shelves will pick up radium diffused from the underlying sediment (Figure 7). The nearshore $^{228}Ra/^{226}Ra$ ratio will be high because newly injected ^{228}Ra will not have decayed to a great extent. However, because of the relatively short half-life of ^{228}Ra (5.77 years), as the water is transported offshore the $^{228}Ra/^{226}Ra$ ratio will decrease because of radioactive decay and mixing with open ocean water containing little ^{228}Ra (radioactive loss of the long-lived ^{226}Ra over the relevant timescales is negligible). This tracer pair therefore provides a sensitive indicator of shelf water in the ocean. This is demonstrated in Figure 8 which shows that the eddy contains a higher $^{228}Ra/^{226}Ra$ ratio than the ambient water, in addition to lower temperature and higher particle content consistent with a shelf-break source.

[14] Because of the known decay rate, the $^{228}Ra/^{226}Ra$ ratio also allows estimation of the rate of shelf-basin exchange. Elapsed time-since-residence on the shelf (T) is derived from the simple radioactive decay equation

$$T = -\ln[R/Ro]\lambda, \quad (1)$$

where λ = decay constant of ^{228}Ra (year^{-1}), R = observed $^{228}Ra/^{226}Ra$ ratio, and Ro is the initial $^{228}Ra/^{226}Ra$ ratio prior to aging. Without knowing the exact source location of the eddy, an initial $^{228}Ra/^{226}Ra$ ratio cannot be precisely assigned and variability of the source either spatially or temporally introduces uncertainty [e.g., *Rutgers van der Loeff et al.*, 2003]. We can, however, estimate the age by comparing shelf values of the $^{228}Ra/^{226}Ra$ ratio with that of the eddy. In Figure 9, $^{228}Ra/^{226}Ra$ ratios from the EHS transects from the SBI July–August 2002 and 2004 cruises are overlaid on the respective temperature sections. The ratios from water samples within the eddy potential density range (26.4–26.8 kg m^{-3}) are highlighted in white. Shelf and shelf break values are in the range 0.86–1.06, while offshore the values drop off to less than 0.7. The trend, however, is not smooth. During the occupation of the sections, XCTD measurements were taken between the water sample casts to increase the spatial resolution. This revealed that the shelf water was being expelled from shelf-break jet as small lenses and filaments. In some of these cold patches the $^{228}Ra/^{226}Ra$ ratios were similar to the higher shelf-break values. For example, near the edge of the 2002 section (Figure 9a) it appears that a deep-reaching, cold-core eddy was present, associated with a very high value of $^{228}Ra/^{226}Ra$ (1.03, although the core of the eddy was missed by the water sample casts).

[15] For the September 2004 cruise, which had a higher sampling rate for radium than the previous cruises, the average $^{228}Ra/^{226}Ra$ ratio from stations 85 and 89 of

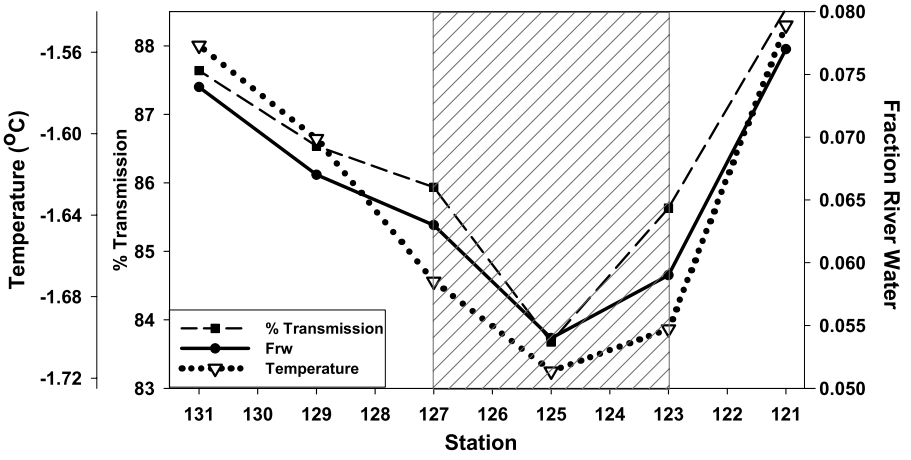

Figure 6. Temperature, percent transmission, and the fraction of river water from the eddy sampling transect (location shown in Figure 2). The hatched region indicates the core of the eddy. The eddy core, though greater than 200 km from the coast, displays properties consistent with nearshore waters.

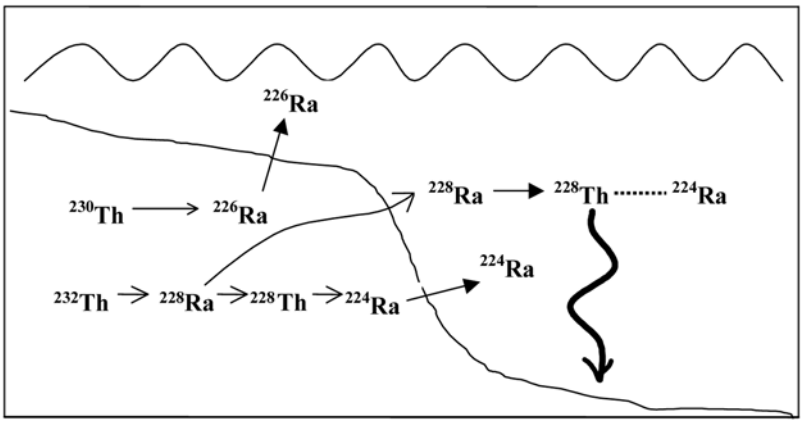

Figure 7. Schematic diagram showing how radium isotopes are produced in the sediments and diffuse into the overlying water. The $^{228}Ra/^{226}Ra$ ratio will decrease as water is transported off the shelf by radioactive decay of ^{228}Ra (5.77 years) and dilution with open ocean water. The long-lived ^{226}Ra is relatively unaffected by these processes. The ^{224}Ra (3.64 days) is produced by ^{228}Th (1.9 years) primarily from sediment as the seawater activity of ^{228}Th is quite low (^{228}Th is particle-reactive and is removed from the water as indicated by the solid wavy line). The ^{228}Th will grow to equilibrium with ^{228}Ra if not removed by particles.

Table 1. Radionuclide Data From USCGC *Healy* Cruise HLY-04-04

Station, Sample Depth (Date)[a]	Latitude, Longitude	Salinity	Temperature, °C	Density	$^{228}Ra/^{226}Ra$	^{224}Ra, dpm/100 L	^{228}Th, dpm/100 L	$^{224}Ra_{xs}$, dpm/100 L
				Eddy Transect				
121, 150 m (9/25/04)	73° 31.42′ N, 160°30.42′W	33.0322	−1.547	26.5749	0.49 ± 0.02	2.03 ± 0.13	1.98 ± 0.06	0.05 ± 0.14
123, 161 m (9/25/04)	73° 28.21′ N, 160°30.30′W	33.1406	−1.696	26.6667	0.84 ± 0.04	1.18 ± 0.12	1.14 ± 0.04	0.04 ± 0.12
125, 171 m (9/25/04)	73° 24.84′N, 160°30.24′W	33.1986	−1.717	26.7143	0.83 ± 0.04	0.87 ± 0.10	1.01 ± 0.08	−0.14 ± 0.13
127, 146 m (9/26/04)	73° 21.71′N, 160°29.76′W	33.1397	−1.673	26.6654	0.81 ± 0.09	1.73 ± 0.10	1.81 ± 0.09	−0.08 ± 0.13
129, 146 m (9/26/04)	73° 18.42′N, 160°29.76′W	33.1726	−1.603	26.6903	0.78 ± 0.09	1.13 ± 0.09	1.30 ± 0.05	−0.17 ± 0.10
131, 135 m (9/26/04)	73° 15.44′N, 160° 29.04′W	33.1426	−1.557	26.6648	0.76 ± 0.05	1.82 ± 0.14	1.67 ± 0.05	0.15 ± 0.15
				Transect 4				
085, 8 m (9/18/04)	72° 56.01′N, 165° 58.74″W	28.9916	3.974	23.0124	1.01 ± 0.09	0.43 ± 0.56	0.22 ± 0.33	0.21 ± 0.07
08502, 30 m (9/18/04)	72° 56.01′N, 165° 58.74″W	32.6102	1.53	26.0907	0.58 ± 0.01	0.39 ± 0.58	0.47 ± 0.38	−0.06 ± 0.07
089, 8 m (9/18/04)	73° 30.36′N, 165° 58.98′W	26.3910	0.3187	21.1531	0.75 ± 0.05	0.79 ± 0.88	0.75 ± 0.38	0.04 ± 0.095
08902, 25 m (9/18/04)	73° 30.36′N, 165° 58.98′W	31.0316	−0.498	24.9224	0.95 ± 0.09	1.02 ± 0.175	0.77 ± 0.13	0.25 ± 0.22
08902, 60 m (9/18/04)	73° 30.36′N, 165° 58.98′W	32.5165	−1.494	26.1595	1.17 ± 0.03	1.47 ± 0.14	1.38 ± 0.09	0.09 ± 0.17
08902, 85 m (9/18/04)	73° 30.36′N, 165° 58.98′W	32.8901	−1.556	26.4597	1.19 ± 0.05	1.90 ± 0.19	0.86 ± 0.06	1.04 ± 0.20
099, 8 m (9/18/04)	74° 27.20′N, 165° 58.74′W	26.6227	1.638	21.2856	0.67 ± 0.05	0.91 ± 0.08	1.10 ± 0.10	−0.19 ± 0.10
				Transect 1				
00202, 8 m (9/6/04)	71° 16.29′N, 152° 11.28′W	28.1663	4.671	22.2942	0.71 ± 0.09	0.79 ± 0.09	0.00 ± 0.06	0.79 ± 0.10
00202, 30 m (9/06/04)	71° 16.29′N, 152° 11.28′W	31.1989	2.023	24.9258	0.97 ± 0.05	1.30 ± 0.11	0.05 ± 0.07	1.25 ± 0.13
00402, 8 m (9/07/04)	71° 21.91′N, 152° 6.72′W	27.9889	4.191	22.1973	1.41 ± 0.16	0.54 ± 0.07	0.00 ± 0.06	0.54 ± 0.09
00402, 25 m (9/07/04)	71° 21.91′N, 152° 6.72′W	31.6839	1.049	25.3767	1.06 ± 0.37	1.41 ± 0.12	0.08 ± 0.12	1.33 ± 0.17
00402, 50 m (9/07/04)	71° 21.91′N, 152° 6.72′W	32.0055	−0.395	25.7057	0.85 ± 0.63	0.14 ± 0.06	0.00 ± 0.005	0.14 ± 0.06
00602, 8 m (9/07/04)	71° 26.86′N, 152° 1.56′W	30.7207	6.066	24.1651	1.13 ± 0.22	0.53 ± 0.06	0.12 ± 0.05	0.41 ± 0.08

Table 1. (continued)

Station, Sample Depth (Date)[a]	Latitude, Longitude	Salinity	Temperature, °C	Density	$^{228}Ra/^{226}Ra$	^{224}Ra, dpm/100 L	^{228}Th, dpm/100 L	$^{224}Ra_{xs}$, dpm/100 L
00602, 50 m (9/07/04)	71° 26.86′N, 152° 1.56′W	31.7344	2.537	25.3651	0.91 ± 0.17	1.28 ± 0.16	0.28 ± 0.16	0.99 ± 0.20
00602, 100 m (9/07/04)	71° 26.86′N, 152° 1.56′W	32.5958	−1.335	26.215	0.92 ± 0.03	0.99 ± 0.12	0.00 ± 0.08	0.99 ± 0.15
00603, 150 m (9/07/04)	71° 26.86′N, 152° 1.56′W	32.8232	−1.630	26.4072	1.07 ± 0.06	1.19 ± 0.10	0.09 ± 0.07	1.09 ± 0.12
00702, 8 m (9/08/04)	71° 29.68′N, 151°59.28′W	28.1662	5.072	22.2552	0.78 ± 0.03	1.06 ± 0.12	0.56 ± 0.07	0.50 ± 0.14
00703, 50 m (9/08/04)	71° 29.68′N, 151°59.28′W	32.1082	−0.358	25.7873	0.93 ± 0.03	0.82 ± 0.11	0.36 ± 0.095	0.45 ± 0.14
00702, 120 m (9/08/04)	71° 29.68′N, 151°59.28′W	32.9875	−1.657	26.5413	0.99 ± 0.02	1.46 ± 0.11	0.11 ± 0.08	1.35 ± 0.14
00703, 250 m (9/08/04)	71° 29.68′N, 151° 59.28′W	34.7127	0.395	27.8523	0.31 ± 0.05	1.05 ± 0.11	0.35 ± 0.09	0.70 ± 0.14
009, 8 m (9/09/04)	71° 34.51′N, 151°55.98′W	29.7229	6.414	23.3369	0.49 ± 0.07	1.60 ± 0.125	1.18 ± 0.07	0.42 ± 0.16
00903, 50 m (9/09/04)	71° 34.51′N, 151°55.98′W	32.221	−0.920	25.9562	0.88 ± 0.10	0.59 ± 0.11	0.44 ± 0.10	0.15 ± 0.15
00903, 100 m (9/09/04)	71° 34.51′N, 151°55.98′W	32.88	−1.575	26.452	0.89 ± 0.06	0.84 ± 0.13	0.46 ± 0.105	0.38 ± 0.17
00902, 200 m (9/09/04)	71° 34.51′N, 151°55.98′W	34.613	0.0695	27.7901	0.12 ± 0.01	1.20 ± 0.13	0.57 ± 0.05	0.63 ± 0.14
015, 8 m (9/10/04)	71° 34.51′N, 151°55.98′W	27.593	4.6556	21.8416	1.00 ± 0.07	0.61 ± 0.10	0.22 ± 0.05	0.38 ± 0.11
01502, 75 m (9/10/04)	71° 50.81′N, 151°42.96′W	33.0019	−1.568	26.5508	1.04 ± 0.09	1.30 ± 0.125	0.49 ± 0.09	0.81 ± 0.15
01502, 150 m (9/10/04)	71° 50.81′N, 151°42.96′W	34.4912	−0.278	27.7098	0.41 ± 0.05	1.58 ± 0.17	0.97 ± 0.14	0.61 ± 0.22
01503, 250 m (9/10/04)	71° 50.81′N, 151°42.96′W	34.7844	0.5186	27.9034	0.15 ± 0.05	0.80 ± 0.07	0.12 ± 0.05	0.68 ± 0.09

[a]Date is given as m/dd/yy.

transect 4 (Figure 4 and Table 1) is 0.94 ± 0.16. This is comparable to the densely sampled transect 1 located east of Barrow Canyon (Figure 10 and Table 1), with an average ratio of 0.98 ± 0.18 within the upper 150 m for stations 2–7. Using the mean of these two shelf-break crossings as an initial value (0.96 ± 0.2), and the eddy ratio of 0.83 ± 0.11, the calculated age of eddy formation on the shelf is 1.1 years with 3.1 years as an upper limit and 0 years as the lower limit.

Table 2. Radium Isotopic Ratios From USCGC *Healy* Cruise HLY-02-03

EHS Section Station	Date[a]	Latitude, Longitude	Sample Depth, m	Station Depth, m	Salinity	Temperature, °C	Density	$^{228}Ra/^{226}Ra$
25	8/06/02	72°14.16′N,159°19.21′W	8	49	31.705	−1.324	25.492	0.65 ± 0.11
25	8/06/02	72°14.16′N,159°19.21′W	38	49	32.992	−1.647	26.54475	0.88 ± 0.05
26	8/06/02	72°35.58′N,158°46.79′W	8	83	29.184	−1.104	23.44374	0.51 ± 0.04
26	8/06/02	72°35.58′N,158°46.79′W	35	83	32.002	−1.442	25.73586	1.03 ± 0.08
26	8/06/02	72°35.58′N,158°46.79′W	71	83	33.045	−1.655	26.58802	1.01 ± 0.05
27	8/07/02	72°42.35′N,158°37.54′W	8	206	28.133	−0.801	22.58709	0.42 ± 0.17
27	8/07/02	72°42.35′N,158°37.54′W	30	206	31.157	−1.528	25.05186	0.65 ± 0.06
27	8/07/02	72°42.35′N,158°37.54′W	110	206	33.123	−1.736	26.65337	0.71 ± 0.23
28	8/08/02	72°50.14′N,158°16.18′W	8	500	27.66	−0.886	22.20607	0.33 ± 0.06
28	8/08/02	72°50.06′N,158°16.84′W	55	488	32.02	−1.528	25.80607	0.89 ± 0.07
28	8/08/02	72°50.14′N,158°16.18′W	120	500	33.023	−1.587	26.56849	0.61 ± 0.04
28	8/08/02	72°50.14′N,158°16.18′W	225	500	34.551	−0.07	27.74785	0.31 ± 0.08
29	8/09/02	72°52.49′N,158°20.69′W	8	1012	27.074	−0.823	21.73101	0.35 ± 0.08
29	8/09/02	72°52.18′N,158°21.14′W	60	1033	32.149	−1.526	25.81659	0.89 ± 0.14
29	8/09/02	72°52.18′N,158°21.14′W	120	1033	33.032	−1.628	26.55245	0.72 ± 0.03
29	8/09/02	72°52.49′N,158°20.69′W	150	1012	33.414	−1.585	26.88609	0.52 ± 0.03
29	8/09/02	72°52.49′N,158°20.69′W	240	1012	34.624	0.169	27.79411	0.14 ± 0.01
30	8/10/02	73°04.56′N,157°54.22′W	8	2037	28.171	−0.661	22.51989	0.55 ± 0.05
30	8/10/02	73°04.21′N,157°56.81′W	70	1998	32.164	−1.396	25.86623	0.91 ± 0.07
30	8/10/02	73°04.21′N,157°56.81′W	110	1998	32.767	−1.541	26.3594	0.65 ± 0.11
30	8/10/02	73°04.56′N,157°54.22′W	150	2037	33.231	−1.524	26.73581	0.47 ± 0.13
30	8/10/02	73°04.56′N,157°54.22′W	240	2037	34.514	−0.17	27.72306	0.43 ± 0.04
31	8/11/02	73°24.07′N,157°31.39′W	8	3041	26.913	−0.361	21.59196	0.42 ± 0.09
31	8/11/02	73°23.68′N,157°33.32′W	60	3021	31.836	−1.055	25.59103	0.77 ± 0.10
31	8/11/02	73°24.07′N,157°31.39′W	150	3041	33.268	−1.642	26.76894	1.03 ± 0.05
31	8/11/02	73°24.07′N,157°31.39′W	250	3041	34.522	−0.159	27.729	0.07 ± 0.25

[a]Date is given as m/dd/yy.

Table 3. Radium Isotopic Ratios From USCGC *Healy* Cruise HLY-04-03

EHS Section Station	Date[a]	Latitude, Longitude	Sample Depth, m	Station Depth, m	Salinity	Temperature, °C	Density	$^{228}Ra/^{226}Ra$
38	8/10/04	72°10.50′N,159°04.70′W	8	50	29.063	−0.29107	23.47155	1.12 ± 0.03
38	8/10/04	72°10.50′N,159°04.70′W	26	50	32.418	−1.56237	26.07645	0.87 ± 0.07
42	8/11/04	72°37.54′N,158°42.44′W	8	115	27.544	0.942226	27.544	0.62 ± 0.06
42	8/11/04	72°37.54′N,158°42.44′W	33	115	32.176	−0.8322	25.85946	1.24 ± 0.08
42	8/11/04	72°37.54′N,158°42.44′W	85	115	33.108	−1.74542	26.64138	0.86 ± 0.09
44	8/11/04	72°42.48′N,158°29.13′W	8	230	27.332	1.288309	21.87105	0.55 ± 0.05
44	8/11/04	72°42.48′N,158°29.13′W	40	230	32.311	−1.43134	25.98639	0.89 ± 0.04
44	8/11/04	72°42.48′N,158°29.13′W	100	230	33.086	−1.73542	26.62326	1.05 ± 0.04
47	8/13/04	72°49.35′N,158°15.24′W	8	420	27.087	3.363807	21.54821	0.93 ± 0.03
47	8/13/04	72°49.14′N,158°16.47′W	55	400	32.441	−1.12827	26.08351	1.10 ± 0.09
47	8/13/04	72°49.35′N,158°15.24′W	110	420	33.128	−1.52537	26.65216	0.49 ± 0.04
47	8/13/04	72°49.35′N,158°15.24′W	170	420	34.568	−0.011	27.75841	0.54 ± 0.14
48	8/14/04	72°54.06′N,158°21.34′W	8	1150	27.732	2.143514	22.1451	0.84 ± 0.04
48	8/14/04	72°53.44′N,158°20.64′W	60	1050	32.468	−1.19829	26.10746	0.94 ± 0.07
48	8/14/04	72°53.44′N,158°20.64′W	115	1050	33.066	−1.72841	26.60685	1.14 ± 0.05
48	8/14/04	72°54.06′N,158°21.34′W	200	1150	34.621	0.169041	27.7916	0.24 ± 0.02
49	8/15/04	73°00.20′N,158°10.51′W	8	1410	27.376	2.483596	21.83958	0.66 ± 0.03
49	8/15/04	72°59.82′N,158°10.31′W	60	1450	32.467	−1.28531	26.10912	0.91 ± 0.09
49	8/15/04	73°00.20′N,158°10.51′W	110	1410	33.081	−1.63539	26.6168	1.05 ± 0.07
49	8/15/04	73°00.20′N,158°10.51′W	190	1410	34.473	−0.26206	27.69437	0.37 ± 0.05
50	8/16/04	73°24.91′N,157°15.24′W	8	3250	26.427	2.507602	21.08066	0.76 ± 0.03
50	8/16/04	73°25.33′N,157°13.20′W	40	3300	30.763	0.030007	24.68576	0.58 ± 0.04
50	8/16/04	73°24.91′N,157°15.24′W	105	3250	32.568	−1.44735	26.19544	0.67 ± 0.03
50	8/16/04	73°24.91′N,157°15.24′W	155	3250	33.084	−1.51636	26.61622	0.89 ± 0.03
51	8/17/04	73°45.18′N,156°47.83′W	8	3600	26.246	0.127	21.081	0.33 ± 0.05
51	8/17/04	73°44.98′N,156°47.60′W	41	3600	31.095	0.995	24.791	0.97 ± 0.04
51	8/17/04	73°45.18′N,156°47.83′W	100	3600	32.475	−1.406	26.196	0.61 ± 0.05
51	8/17/04	73°45.18′N,156°47.83′W	150	3600	33.013	−1.542	26.616	1.34 ± 0.08

[a]Date is given as m/dd/yy.

Certainly, the age of formation was well within the decay time of ^{228}Ra. To better constrain this, shorter lived tracers prove useful.

3.2.2. Radium-224

[16] The short-lived isotope ^{224}Ra ($T_{1/2}$ = 3.64 days) has only recently been measured in the Arctic Ocean but was shown to have utility for studying rapid, short-timescale processes over the shelves [*Kadko and Muench*, 2005]. The ^{224}Ra is produced from decay of ^{228}Th, which is itself produced by ^{228}Ra. The ^{228}Th is concentrated in sediments and, owing to its high particle reactivity, has only a small activity in coastal waters. In such cases the seawater activity ratio of $^{228}Th/^{228}Ra$ is typically <0.05 [e.g., *Kaufman et al.*, 1981], so nearshore background ^{224}Ra from seawater ^{228}Th

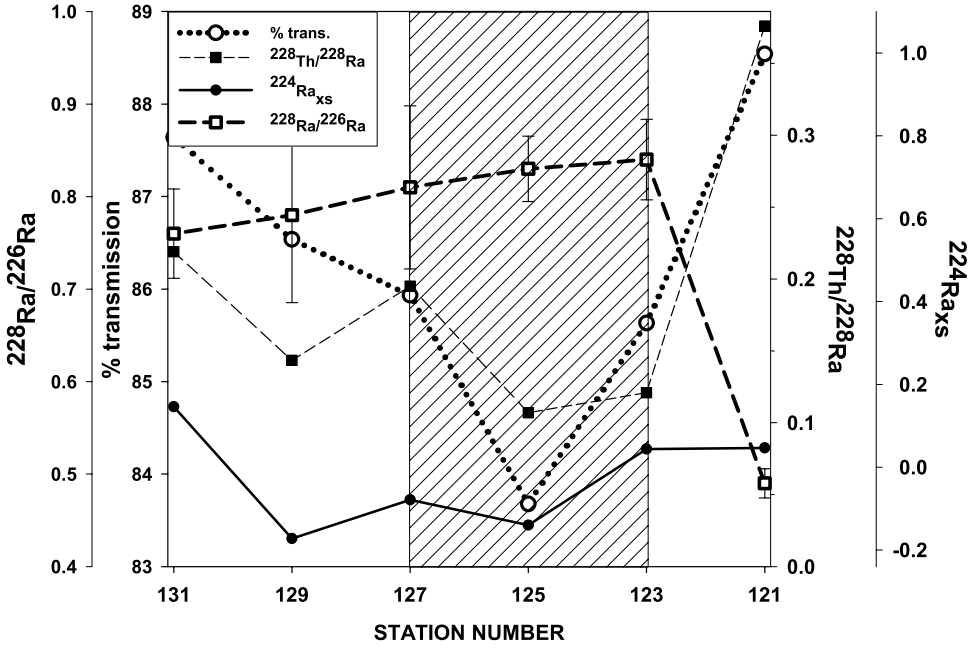

Figure 8. The $^{228}Ra/^{226}Ra$, $^{224}Ra_{xs}$, percent light transmission, and $^{228}Th/^{228}Ra$ from the hydrographic transect through the center of the eddy (location shown in Figure 2). The hatched region indicates the core of the eddy.

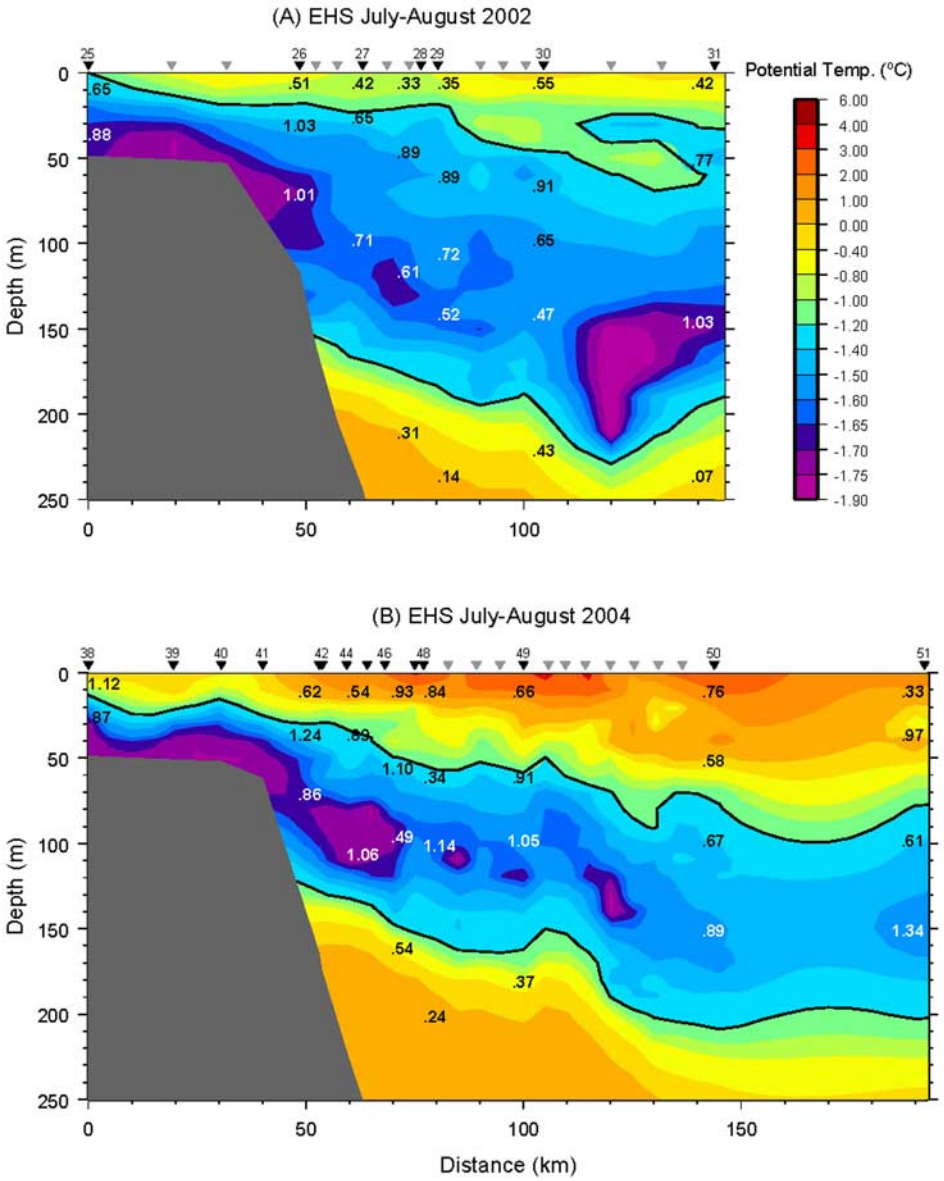

Figure 9. The $^{228}Ra/^{226}Ra$ ratios overlaid on potential temperature (°C, color) for the EHS transects in July–August (a) 2002 and (b) 2004. Ratios for water within the density range of the eddy are highlighted in white. The −1.2°C isotherm is contoured, which approximately delimits the newly ventilated layer (used for Figure 13a). The black numbered inverted triangles denote the CTD stations, and the grey inverted triangles denote the XCTD sites.

will be small compared to that diffusing from the shelf sediments. The ^{224}Ra activity above the background ^{228}Th activity is defined as excess ^{224}Ra ($^{224}Ra_{xs} = {}^{224}Ra_{total} - {}^{228}Th$), and will decay to zero once the water parcel is removed from sediment contact. The short half-life of ^{224}Ra dictates that $^{224}Ra_{xs}$ will not be observed far offshore and is therefore a useful tracer of rapid cross-shelf transport processes.

[17] Figure 10 shows the $^{224}Ra_{xs}$, ^{228}Th and percent light transmission data from transect 1 in September 2004, along with the potential temperature and salinity sections. There is high $^{224}Ra_{xs}$ nearshore, including a maximum coincident with the shelf-break temperature minimum at station 7 near 125 m depth. This corresponds to the eastward flowing shelf-break jet, which at the time of occupation of the section contained winter-transformed Pacific water [*Pickart*, 2004; *Pickart et al.*, 2005; *Nikolopoulos et al.*, 2008]. Note that this short-lived isotope decreased in activity offshore of the boundary current. Within the eddy feature, $^{224}Ra_{xs}$ is absent (Figure 8) indicating that the feature had not been in contact with shelf sediments for at least 2 weeks.

3.2.3. The $^{228}Th/^{228}Ra$ Tracer

[18] As discussed above, particle rich coastal waters will have very low $^{228}Th/^{228}Ra$ ratios. In the example from transect 1 (Figure 10) the nearshore $^{228}Th/^{228}Ra$ ratios are in the range 0–0.05 indicative of active scavenging of ^{228}Th within the particle-rich coastal area. Water offshore has much higher $^{228}Th/^{228}Ra$ ratios. It follows that an eddy

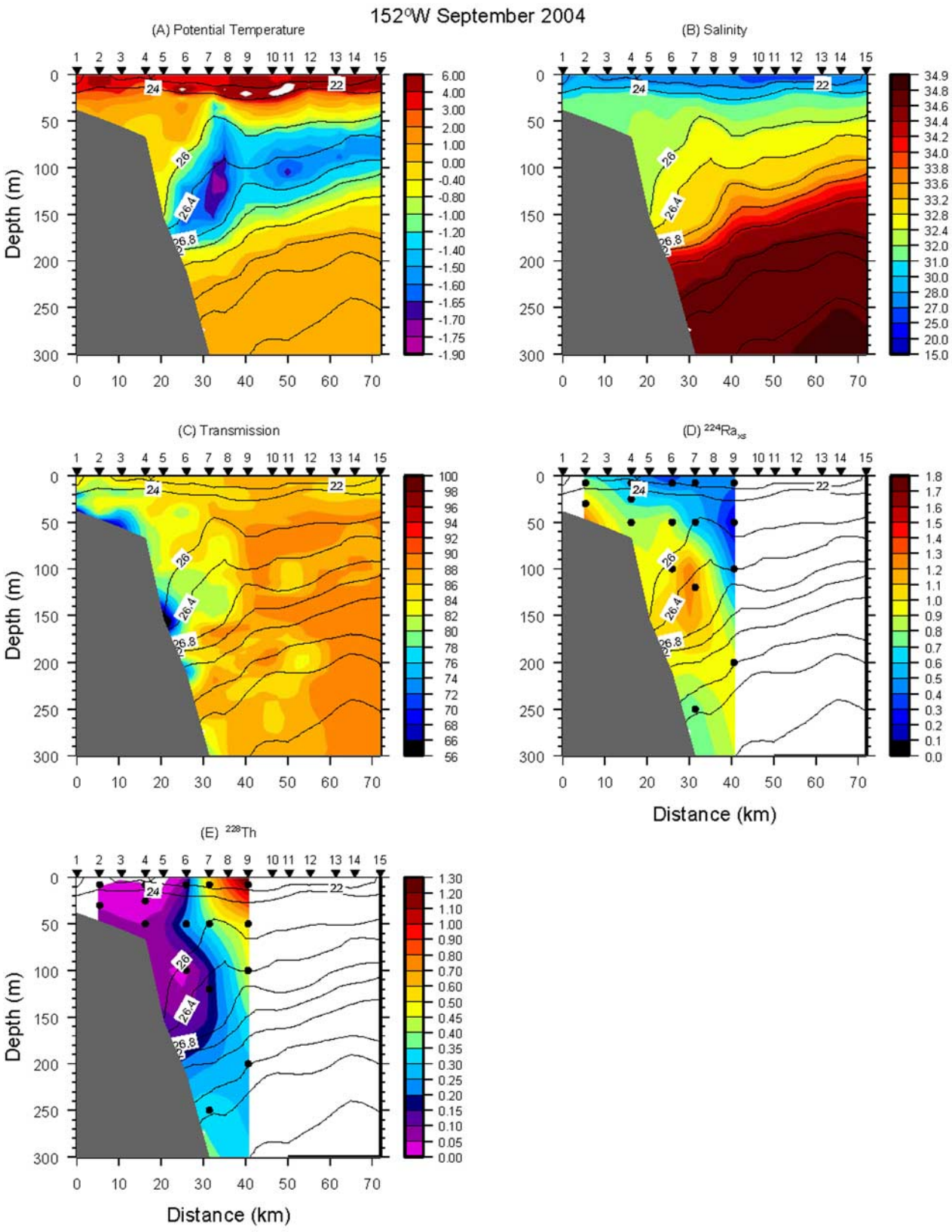

Figure 10. Property sections from transect1 of the September 2004 USCGC *Healy* cruise HLY-04-04 (see Figure 1 for location). In each plot the contours are potential density (kg m^{-3}). The closed circles denote the sample locations of the radioisotopes. (a) Potential temperature (°C), (b) salinity, (c) percent transmission, (d) $^{224}Ra_{xs}$, and (e) ^{228}Th. Isotope units are in dpm/100 L.

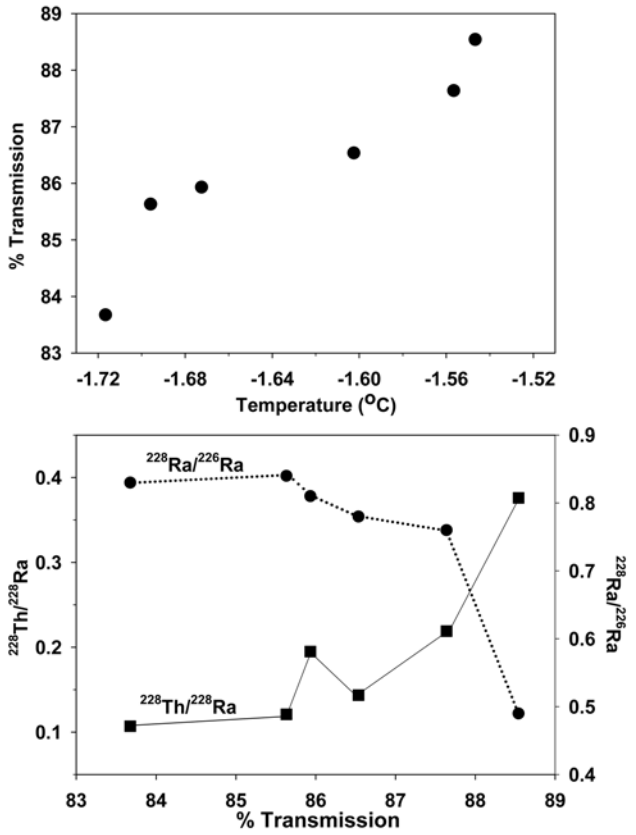

Figure 11. (top) Light transmission plotted against temperature for eddy hydrographic transect samples. The cold temperatures and low-percent transmission correspond to the eddy core. (bottom) Plots of $^{228}Ra/^{226}Ra$ ratios and $^{228}Th/^{228}Ra$ ratios against percent transmission for the eddy hydrographic transect contrasting the shelf characteristics of the eddy with ambient water.

formed from the shelf-break environment would capture the low $^{228}Th/^{228}Ra$ signal, as did the eddy in this study (Figure 8). As the eddy moves offshore the $^{228}Th/^{228}Ra$ would be expected to increase given adequate time for ^{228}Th ingrowth ($T_{1/2}$ = 1.9 years) and no additional loss of ^{228}Th within the migrating eddy. The latter condition would be met if little particle loss occurred in the eddy. This appears to be the case when comparing the light transmission data between the shelf and eddy where the eddy core had a value of 83–84% comparable to values typically observed near the shelf break (Figures 3 and 4). Similarly, the particulate organic carbon (POC) concentrations of the eddy (1–4 μmol/L) are comparable to shelf-break values ranging from 1–3 μmol/L in spring 2004 and 1–10 μmol/L in summer 2004 [*Bates et al.*, 2005]. If the initial $^{228}Th/^{228}Ra$ = 0, then as an upper limit the age of the eddy would be 3 months. This would be a lower limit if active loss of ^{228}Th is occurring. The contrast of the shelf isotopic characteristics of the eddy with ambient water is summarized in Figure 11.

3.3. Comparison to Oxygen Utilization Rate

[19] The utility of radioactive elements to trace rates of oceanographic processes stems from known decay rates which are physical constants, independent of chemical and biological conditions of the environment. Other time-dependent tracers, such as oxygen, can provide a semiquantitative measure of elapsed time if suitable rate constants are measured. During the SBI program, a limited number of deep respiration rate measurements were made in slope and shelf waters ranging in depth from 75 to 200 m. The value obtained was 0.008 ± 0.003 mL/L/d (M. Cottrell, personal communication, 2007). Using this value, it is possible to estimate an eddy age by comparing the difference in O_2 between the source and eddy.

[20] Without knowing the precise location of the eddy source, we use as an example the low-temperature winter-transformed water over the shelf and shelf break previously discussed for transect 4 (Figure 4). As seen in Figure 12a, the oxygen content of the water in question (colder than −1.7°C within the density layer of the eddy) ranges from 6.25 to 7.3 mL/L. However, the water directly in contact with the bottom (stations 91–93 in Figure 4, associated with very low values of transmissivity) is likely lower in oxygen because of enhanced benthic activity and not representative of an initial oxygen level. We use the range of 6.75–7.3 mL/L for the eddy source water. Note in Figure 12a that a high-oxygen (7.3 mL/L) cold-core eddy was in the process of being formed from the shelf-break jet when the section was occupied (stations 97–98). The eddy feature that we sampled with the high-resolution survey (farther to the east and offshore of transect 4) also contained high oxygen in its core (Figure 12b), but the O_2 concentration was lower, approximately 6.72 mL/L. On the basis of the measured respiration rate, this suggests an eddy age in the range of 0–70 days, which is consistent with the results derived from the radionuclide evaluation.

4. Summary and Implications

[21] The radioisotope evaluation of the cold core anticyclonic eddy sampled in September 2004 suggests that its age-since-formation over the shelf environment was on the order of months. This is consistent with oxygen levels within the eddy and with the presence of elevated abundances of Calanus glacialis copepodites (juvenile stages) inside the feature, suggesting the eddy must have formed earlier that spring or summer. Calanus glacialis has an annual cycle and reproduces during spring and summer only [*Llinás et al.*, 2008; L. Llinás, personal communication, 2007]. This is also consistent with the water mass in the eddy core, winter-transformed Chukchi/Bering water, which is typically found in the shelf-break current from early spring to early fall. Note that while each of the age techniques used in this study is associated with a degree of uncertainty, the fact that all of the methods give consistent results implies that the estimate of several months is robust.

[22] It appears that over this timeframe substantial aging in regards to initial concentrations of substances critical to biogeochemical cycles did not occur. At the edge of the deep basin the eddy was poised to deliver biogeochemically significant shelf material to the central Arctic. For example, Figure 13 compares the DOC distribution inside the eddy core with that of the shelf, and there appears to have been little utilization of the DOC within this timescale in contrast

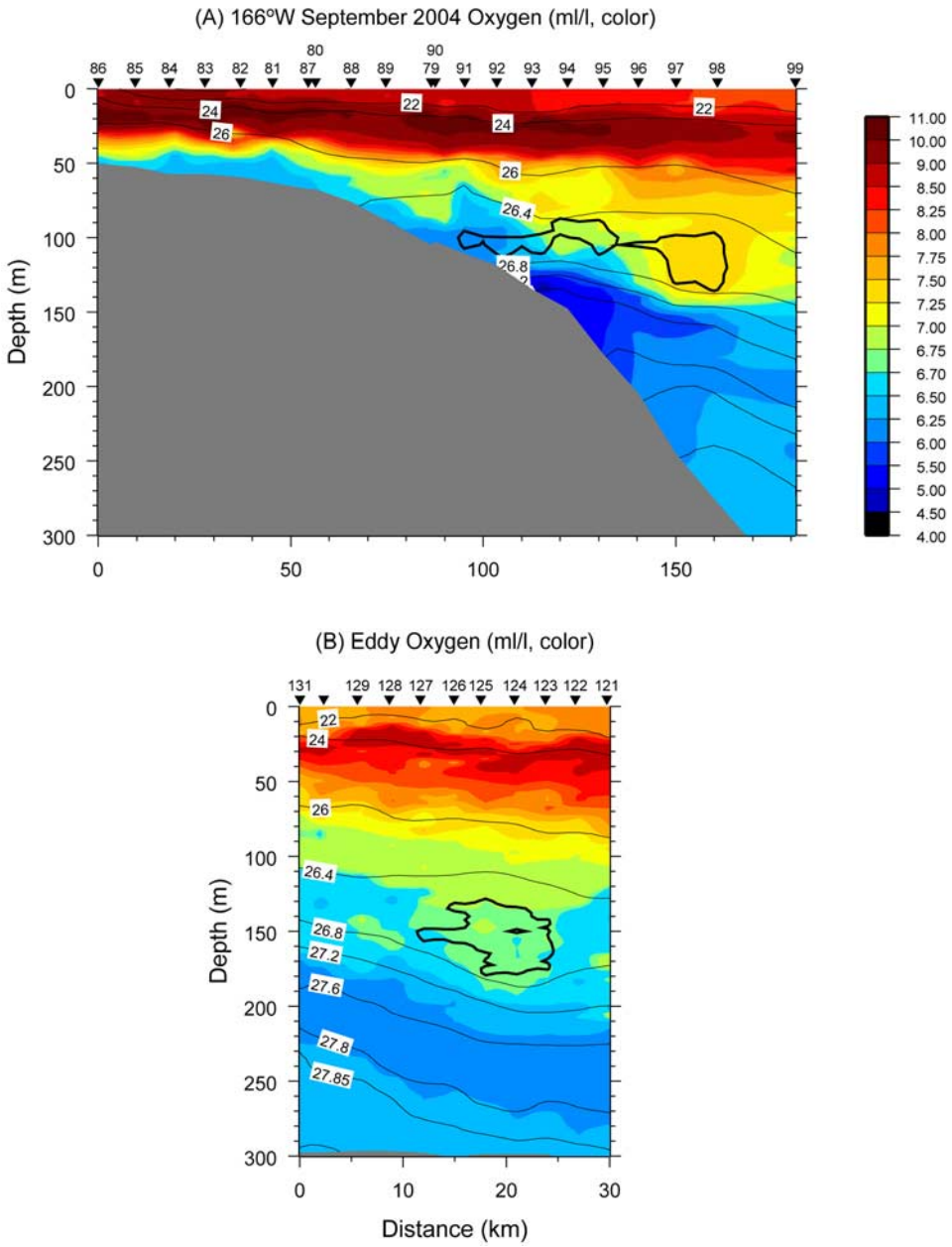

Figure 12. (a) Oxygen concentration (mL/L, color) overlaid with potential density (kg m^{-3}, contours) across transect 4 occupied during the September 2004 USCGC *Healy* cruise HLY-04-04. This is the same section shown in Figure 4. The thick, dark lines delimit the winter water colder than −1.7°C from Figure 4, left plot. (b) Vertical section of oxygen (mL/L, using the same color bar as in Figure 12a overlaid with potential density (contours) across the eddy. The thick, dark lines delimit the water colder than −1.7°C from the eddy potential temperature section of Figure 3, left plot.

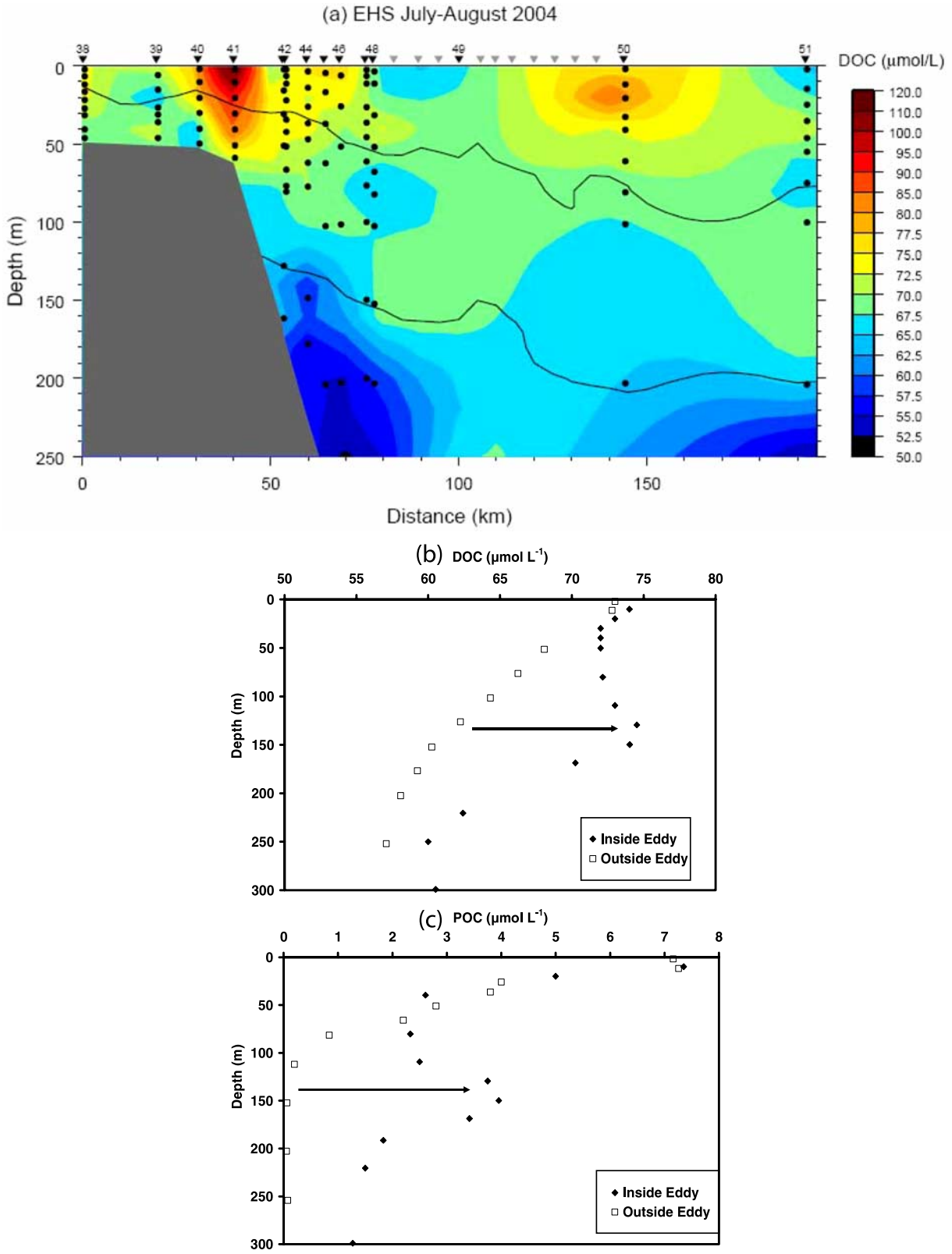

Figure 13. (a) Vertical section of DOC (color, μmol/L) overlaid with potential density (contours, kgm^{-3}) from the EHS transect July–August 2004 (the corresponding potential temperature section is shown in Figure 9b). The thick, dark lines are the -1.2°C isotherm from Figure 9b. Note that DOC is enhanced in the vicinity of the shelf break, where the eddy was likely formed, compared to the low-DOC environment of the deep basin. This trend is consistent with the radium and temperature distributions shown in Figure 9. (b) DOC and (c) POC distributions inside the eddy core from September 2004 compared to ambient water.

to the very low concentrations in the ambient water surrounding the eddy. Similarly, the nutrient and high-POC signal transported within the eddy from the shelf break was conserved [*Mathis et al.*, 2007]. The presence of the shelf species *Pseudocalanus* spp. within the eddy suggests that planktonic forms may also persist for several months within the eddy with subsequent availability for transport to the central basin. Observations of *Pseudocalanus* spp. from central parts of the basin reported elsewhere could represent populations carried offshore by such eddies. These populations may survive temporarily by feeding under ice but it is unlikely that they can be sustained indefinitely in basin waters. The absence or patchiness of the genus in some surveys in the more central parts of the basin could reflect variability in the mesoscale processes responsible for its transport from the continental shelves [*Llinás et al.*, 2008].

[23] The survey performed here represented a single snapshot of an eddy in the western Arctic, as time constraints precluded investigating the evolution of the feature with repeat analyses. A logical follow up to this work would be to track such an eddy over a period of time and perform time series surveys to test the dating methods, as well as to examine the spin-down and chemical and biological evolution of the feature as it becomes incorporated into the central basin.

[24] **Acknowledgments.** This work was supported by National Science Foundation Polar Programs grants OPP-662690 and OPP-66040N to the University of Miami (DK), and Office of Naval Research grant N00014-02-1-0317 (RP). We extend thanks to M. Stephens for field and laboratory assistance, L. Llinás for helpful discussions on zooplankton distributions, M. Cottrell for providing deep respiration data, L. Cooper for ^{18}O analysis of the eddy, and the crew of the research icebreaker USCGC *Healy* for their capable and enthusiastic field support.

References

Aagaard, K., and E. C. Carmack (1994), The Arctic Ocean and climate: A perspective, in *The Polar Oceans and Their Role in Shaping the Global Environment*, *Geophys. Monogr. Ser.*, vol. 85, edited by O. M. Johannessen, R. D. Muench, and J. E. Overland, pp. 5–20, AGU, Washington, D. C.

Bates, N. R., D. Hansell, S. B. Moran, and L. A. Codispoti (2005), Seasonal and spatial distribution of particulate organic matter (POM) in the Chukchi and Beaufort Sea, *Deep Sea Res., Part II*, *52*, 3324–3343.

Coachman, L. K., and K. Aagaard (1966), Transports through Bering Strait: Annual and interannual variability, *J. Geophys. Res.*, *93*, 15,535–15,539.

Cooper, L. W., T. E. Whitledge, J. M. Grebmeier, and T. Weingartner (1997), The nutrient, salinity, and stable isotope composition of Bering and Chukchi seas waters in and near Bering Strait, *J. Geophys. Res.*, *102*, 12,563–12,573.

D'Asaro, E. A. (1988a), Generation of submesoscale vortices: A new mechanism, *J. Geophys. Res.*, *93*, 6685–6693.

D'Asaro, E. A. (1988b), Observations of small eddies in the Beaufort Sea, *J. Geophys. Res.*, *93*, 6669–6684.

Hansell, D. A., D. Kadko, and N. R. Bates (2004), Non-conservative behavior of terrigenous dissolved organic carbon in the western Arctic Ocean, *Science*, *304*, 858–861.

Kadko, D., and R. Muench (2005), Evaluation of shelf-basin interaction in the western Arctic by us of short-lived radium isotopes: The importance of mesoscale processes, *Deep Sea Res., Part II*, *52*, 3227–3244.

Kadko, D., and P. Swart (2004), The source of the high heat and freshwater content of the upper ocean at the SHEBA site in the Beaufort Sea in 1997, *J. Geophys. Res.*, *109*, C01022, doi:10.1029/2002JC001734.

Kaufman, A., Y.-H. Li, and K. K. Turekian (1981), The removal rates of ^{234}Th and ^{228}Th from waters of the New York Bight, *Earth Planet. Sci. Lett.*, *54*, 384–392.

Llinás, L., R. S. Pickart, J. T. Mathis, and S. L. Smith (2008), Zooplankton inside an Arctic Ocean cold-core eddy: Probable origin and fate, *Deep Sea Res., Part II*, in press.

Macdonald, R. W., D. W. Paton, E. C. Carmack, and A. Omstedt (1995), The freshwater budget and under-ice spreading of Mackenzie river water in the Canadian Beaufort Sea based on salinity and $^{18}O/^{16}O$ measurements in water and ice, *J. Geophys. Res.*, *100*, 895–919.

Macdonald, R. W., E. C. Carmack, F. A. McLaughlin, K. K. Kalkner, and J. H. Swift (1999), Connections among ice, runoff and atmospheric forcing in the Beaufort Gyre, *Geophys. Res. Lett.*, *26*, 2223–2226.

Manley, T. O., and K. Hunkins (1985), Mesoscale eddies of the Arctic Ocean, *J. Geophys. Res.*, *90*, 4911–4930.

Mathis, J. T., R. S. Pickart, D. A. Hansell, D. Kadko, and N. R. Bates (2007), Eddy transport of organic carbon and nutrients from the Chukchi Shelf: Impact on the upper halocline of the western Arctic Ocean, *J. Geophys. Res.*, *112*, C05011, doi:10.1029/2006JC003899.

Michel, J., W. S. Moore, and P. T. King (1981), γ-Ray spectrometry for determination of radium-228 and radium-226 in natural waters, *Anal. Chem.*, *53*, 1885–1889.

Moore, W. S., and R. Arnold (1996), Measurement of ^{223}Ra and ^{224}Ra in coastal waters using a delayed coincidence counter, *J. Geophys. Res.*, *101*, 1321–1329.

Moore, W. S., R. M. Key, and J. L. Sarmiento (1985), Techniques for precise mapping of ^{226}Ra and ^{228}Ra in the ocean, *J. Geophys. Res.*, *90*, 6983–6994.

Muench, R. D., J. T. Gunn, T. E. Whitledge, P. Schlosser, and W. S. Smethie Jr. (2000), An Arctic Ocean cold-core eddy, *J. Geophys. Res.*, *105*, 23,997–24,006.

Münchow, A., E. C. Carmack, and D. A. Huntley (2000), Synoptic density and velocity observations of slope waters in the Chukchi and East-Siberian Seas, *J. Geophys. Res.*, *105*, 14,103–14,119.

Newton, J. L., K. Aagaard, and L. K. Coachman (1974), Baroclinic eddies in the Arctic Ocean, *Deep Sea Res.*, *21*, 707–719.

Nikolopoulos, A., R. S. Pickart, P. S. Fratantoni, K. Shimada, D. J. Torres, and E. P. Jones (2008), The Western Arctic Boundary Current at 152W: Structure, variability, and transport, *Deep Sea Res., Part II*, in press.

Orr, J. C., N. L. Guinasso Jr., and D. R. Schink (1985), Radon surpluses in warm core rings, *J. Geophys. Res.*, *90*, 8903–8916.

Padman, L., M. Levine, T. Dillon, M. Morison, and J. Pinkel (1990), Hydrography and microstructure of an Arctic cyclonic eddy, *J. Geophys. Res.*, *95*, 9411–9420.

Pickart, R. S. (2004), Shelfbreak circulation in the Alaskan Beaufort Sea: Mean structure and variability, *J. Geophys. Res.*, *109*, C04024, doi:10.1029/2003JC001912.

Pickart, R. S., T. J. Weingartner, L. J. Pratt, S. Zimmermann, and D. J. Torres (2005), Flow of winter-transformed Pacific water into the western Arctic, *Deep Sea Res., Part II*, *52*, 3175–3198.

Rutgers van der Loeff, M. M., R. M. Key, J. Scholten, D. Bauch, and A. Michel (1995), ^{228}Ra as a tracer for shelf water in the Arctic Ocean, *Deep Sea Res., Part II*, *42*, 1533–1553.

Rutgers van der Loeff, M., S. Kuhne, M. Wahsner, H. Holtzen, M. Frank, B. Ekwurzel, M. Mensch, and V. Rachold (2003), ^{228}Ra and ^{226}Ra in the Kara and Laptev seas, *Cont. Shelf Res.*, *23*, 113–124.

Spall, M. A. (2007), Circulation and water mass transformation in a model of the Chukchi Sea, *J. Geophys. Res.*, *112*, C05025, doi:10.1029/2005JC003364.

Spall, M. A., R. S. Pickart, P. S. Fratantoni, and A. J. Plueddemann (2008), Western Arctic shelfbreak eddies: Formation and transport, *J. Phys. Oceanogr.*, in press.

Weingartner, T., K. Aagaard, R. Woodgate, S. Danielson, Y. Sasaki, and D. Cavalieri (2005), Circulation on the north central Chukchi Sea shelf, *Deep Sea Res., Part II*, *52*, 3150–3174.

Winsor, P., and D. C. Chapman (2004), Pathways of Pacific water across the Chukchi Sea: A numerical model study, *J. Geophys. Res.*, *109*, C03002, doi:10.1029/2003JC001962.

Woodgate, R. A., K. Aagaard, and T. Weingartner (2005), A year in the physical oceanography of the Chukchi Sea: Moored measurements from autumn 1990–1991, *Deep Sea Res., Part II*, *52*, 3116–3149.

D. Kadko and J. Mathis, Rosenstiel School of Marine and Atmospheric Science, University of Miami, 4600 Rickenbacker Causeway, Miami, FL 33149-1098, USA. (dkadko@rsmas.miami.edu)

R. S. Pickart, Woods Hole Oceanographic Institution, MS 21, Woods Hole, MA 02543, USA.